
Multi-Step Knowledge Interaction Analysis via Rank-2 Subspace Disentanglement

Sekh Mainul Islam¹ Pepa Atanasova¹ Isabelle Augenstein¹

Abstract

Natural Language Explanations (NLEs) describe how Large Language Models (LLMs) make decisions by drawing on external Context Knowledge (CK) and Parametric Knowledge (PK). Understanding the interaction between these sources is key to assessing NLE grounding, yet these dynamics remain underexplored. Prior work has largely focused on i) single-step generation and ii) modelled PK–CK interaction as a binary choice within a rank-1 subspace. This approach overlooks richer interactions and how they unfold over longer generations, such as complementary or supportive knowledge. We propose a novel rank-2 projection subspace that disentangles PK and CK contributions more accurately and use it for the first multi-step analysis of knowledge interactions across longer NLE sequences. Experiments across four QA datasets and three open-weight LLMs demonstrate that while rank-1 subspaces struggle to represent diverse interactions, our rank-2 formulation captures them effectively, highlighting PK alignment for supportive interactions and CK alignment for conflicting ones. Our multi-step analysis reveals among others that hallucinated generations exhibit strong alignment with the PK direction, whereas context-faithful generations maintain a more balanced alignment between PK and CK¹.

process for predictions in complex reasoning tasks such as Claim Verification (CV) and Question Answering (QA). These NLEs are valuable because they can reveal the utilization of external context and the knowledge stored in model parameters. Consider the Figure 1 example from a QA task (Cheng et al., 2024), where Llama-3.1-8B-Instruct (Meta-Team, 2024) generates the NLE by utilizing both Context Knowledge (CK) and Parametric Knowledge (PK), to explain the underlying decision-making process for the final answer prediction. For some tasks, such as CV, we assume the decision-making process and, in turn, the NLE, will rely more on evidence (CK) (Wang & Shu, 2023; Tan et al., 2025), and in QA tasks with misleading external context, we assume they will rely on the PK. On the other hand, Chain-of-Thought (CoT) prompting (Wei et al., 2022), a widely adopted reasoning methodology, explicitly elicits NLEs of the intermediate reasoning steps and is hypothesized to influence how LLMs integrate PK and CK (Cheng et al., 2024; Su et al., 2024; Tao et al., 2025), potentially improving contextual grounding. However, it remains unclear what the learned PK-CK interaction dynamics in generating the NLEs are, *necessitating a multi-step analysis of PK-CK interaction across longer NLE sequences.*

Prior work (Longpre et al., 2021; Xu et al., 2024; Minder et al., 2025) has primarily focused on uncovering the single-step generation mechanism – typically the final answer, and modelled only conflicting PK–CK interaction as a binary choice in a rank-1 subspace, thereby overlooking richer forms such as complementary or supportive knowledge (Cheng et al., 2024). We thus hypothesize that this *rank-1 subspace is not sufficient to disentangle the individual contributions of PK and CK in all types of knowledge interaction scenarios.* Moreover, they did not characterize the step-by-step PK-CK interaction dynamics over longer sequences, such as NLE generation for different knowledge interactions. To accurately understand the knowledge interaction dynamics during NLE generation, we investigate the following research questions:

RQ1. *Is a rank-1 projection subspace enough for disentangling PK and CK contributions in all types of knowledge interaction scenarios?*

RQ2. *How do individual PK and CK contributions change*

1. Introduction

Large Language Models (LLMs) are employed to generate Natural Language Explanations (NLEs) in a human-readable format, illustrating the underlying decision-making

¹Department of Computer Science, University of Copenhagen, Copenhagen, Denmark. Correspondence to: Sekh Mainul Islam <seis@di.ku.dk>.

Preprint. February 2, 2026.

¹Code and data: <https://github.com/copenlu/pk-ck-knowledge-disentanglement>

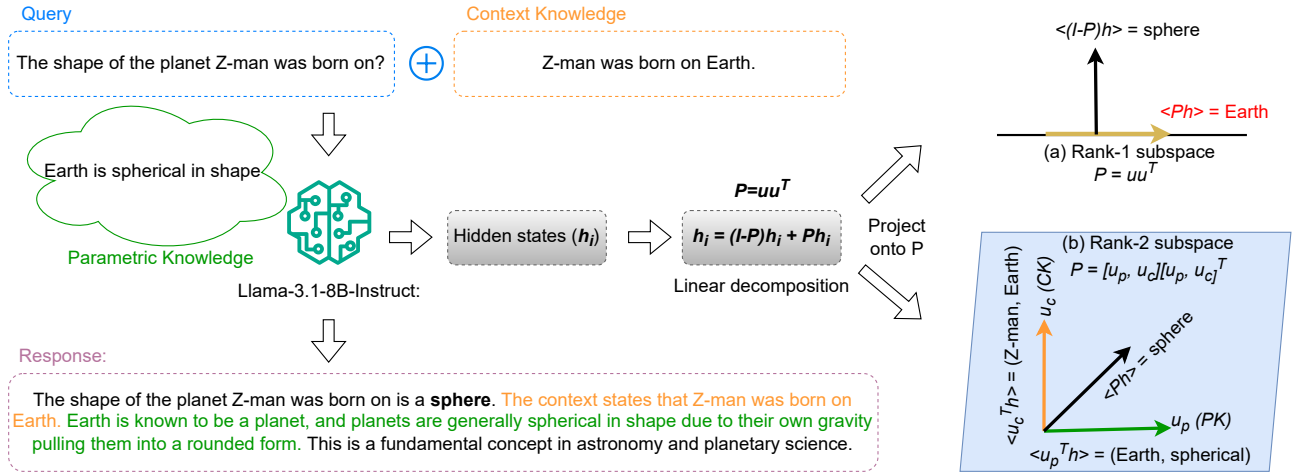


Figure 1. (Left) Llama-3.1-8B-Instruct model combines parametric (green) and contextual (orange) knowledge to generate NLEs. (Right) Projection of the answer token to a learned low-rank subspace \mathbf{P} disentangles their contributions – (a) rank-1 fails to disentangle individual knowledge contributions and its orthogonal subspace encodes the correct knowledge, whereas (b) rank-2 successfully encodes the correct knowledge and disentangles individual knowledge contributions.

over the NLE generation steps for different knowledge interactions?

RQ3. Can we find reasons for hallucinations based on PK-CK interactions?

RQ4. How is the CoT mechanism aligned with the knowledge interaction subspace?

We perform experiments on four publicly available QA datasets for three open-weight instruction-tuned LMs. In RQ1 (§4.2), we find that the rank-1 subspace (Minder et al., 2025) fails to disentangle individual knowledge contributions for different knowledge interactions. For RQ2 (§4.3), using a more accurate rank-2 subspace disentanglement, we find that, during NLE generation, the model utilizes both knowledge sources with slight prioritization of PK; towards the final answer generation, the model aligns closely with the CK direction for conflicting examples; for supportive examples, it aligns more with the PK direction. This learned rank-2 subspace also illustrates PK dominance for the sequences with hallucinated spans (RQ3, §4.4). Finally, for the RQ4 (§4.5), we observe that the CoT mechanism is also encoded in the LLM as a low-rank space, and the CoT encoding subspace closely aligns with the context direction of the rank-2 knowledge interaction subspace. Overall, this work advances understanding of how LLMs integrate internal and external knowledge by introducing the first systematic framework for multi-step analysis of knowledge interactions via rank-2 subspace disentanglement.

2. Related Work

Parametric vs. contextual knowledge in LMs. A large body of work studies what language models encode as *para-*

metric knowledge (PK) and how they integrate *contextual knowledge (CK)* at inference time (Petroni et al., 2019; Jiang et al., 2020; Roberts et al., 2020; Hagström et al., 2025; Marjanovic et al., 2024; Yu et al., 2024). Early work showed that factual knowledge can be elicited directly from model parameters (Petroni et al., 2019), while probing and representation analyses examined how context and memory are encoded and combined across layers (Brown et al., 2020; Tenney et al., 2019; Bi et al., 2025).

More recent studies focus on PK–CK interaction and conflict. Cheng et al. (2024) analyzed suppression effects between PK and CK under different interaction regimes, while Xu et al. (2024) categorized conflict types (context–memory, inter-context, intra-memory) and their behavioral consequences. Several approaches aim to improve PK–CK balance through training or inference-time interventions, including enhanced pretraining or fine-tuning (Zhang et al., 2024), context-aware representation manipulation (Yuan et al., 2025b), contrastive decoding (Zhao et al., 2024), and lightweight steering methods that increase context sensitivity without weight updates (Wang et al., 2025). Our work complements this line by introducing a geometric framework that disentangles PK and CK in a rank-2 subspace and enables multi-step analysis during generation.

Natural language explanations and reasoning. Natural Language Explanations (NLEs) are widely used to expose or guide model reasoning in complex tasks (Camburu et al., 2018; Atanasova et al., 2020). Explanation-based supervision improves QA performance (Rajani et al., 2019), and Chain-of-Thought (CoT) prompting elicits stepwise reasoning that enhances multi-hop and arithmetic reasoning (Wei et al., 2022; Lampinen et al., 2022). However, multiple

studies show that NLEs and CoT are often unfaithful to the model’s true decision process, functioning as post-hoc rationalizations rather than causal explanations (Atanasova et al., 2023; Turpin et al., 2023; Siegel et al., 2024; Yuan et al., 2025a; Wang & Atanasova, 2025). Our work addresses this gap by providing a token-level, representation-based analysis of how PK and CK jointly shape NLE generation, linking explanation faithfulness and hallucination to internal knowledge alignment.

Probing, subspaces, and identifiability. Probing methods reveal that linguistic and factual properties are encoded in low-dimensional subspaces of LM representations (Hewitt & Manning, 2019; Clark et al., 2019). The superposition hypothesis further suggests that multiple features are compressed into overlapping linear subspaces (Elhage et al., 2022). Building on this view, Minder et al. (2025) modeled PK–CK conflict using a single controllable direction (rank-1 subspace). However, when PK and CK are jointly encoded, such a representation is non-identifiable and cannot disentangle individual contributions. We generalize this approach to a rank-2 projection subspace, establishing identifiability and enabling fine-grained, multi-step analysis of PK–CK interaction dynamics during generation.

3. Method

3.1. Task Formulation

Let \mathcal{Q} and \mathcal{C} denote two disjoint sets of queries and contexts, respectively, and consider a QA dataset $\mathcal{D} \subseteq \mathcal{Q} \times \mathcal{C}$. For a question–context pair $(q, c) \in \mathcal{D}$, with $q \in \mathcal{Q}$ and $c \in \mathcal{C}$, a language model p generates both an answer a and an NLE with n tokens as $\mathcal{E} = \{e_i\}_{i=1}^n$. We distinguish between three forms of answer generation: (i) the parametric answer $a(q, \phi)$, produced by recalling PK (independent of c , ϕ denotes no context), (ii) the contextual answer $a(q, c)$, obtained by leveraging the provided context while disregarding parametric recall, and (iii) the final predicted answer a combining both the provided context and the PK recall guided by the PK–CK knowledge interaction.

During the sequential generation of \mathcal{E} , each token e_i is influenced by the interaction between $a(q, \phi)$ and $a(q, c)$. This evolving interaction guides the generation of NLE \mathcal{E} , illustrating the decision-making process of the final predicted answer a . To analyze this process, we quantify the contribution of parametric knowledge (α_i^p) and contextual knowledge (α_i^c) at each generation step i , and we define their difference as

$$\Delta_i = \alpha_i^p - \alpha_i^c, i \in [1, n] \quad (1)$$

By tracking Δ_i across all NLE generation steps, we aim to characterize the interaction and the shifting balance between parametric and contextual sources throughout NLE

generation.

3.2. Identify Different PK–CK Interactions

To characterize different types of PK–CK interactions guided by individual knowledge contribution, we draw from Minder et al. (2025), who analyze intent-driven answer control, i.e., controlling the model towards a specific answer generation aligned with the intent of following either PK or CK. Let w_c (instruction to follow the CK only) and w_p (instruction to follow the PK only) denote intents toward predicting $a(q, c)$ and $a(q, \phi)$, respectively, for a given (q, c) .

Minder et al. (2025) restrict intent to conflicting cases, where $a(q, c) \neq a(q, \phi)$ and the final answer a is determined by either w_c or w_p . We generalize this, following Cheng et al. (2024), to encompass a broader set of interactions:

- Supportive: $a(q, c) = a(q, \phi) = a$; PK and CK reinforce the same outcome, leading to high confidence in the prediction.
- Complementary: $a(q, c) \neq a(q, \phi)$ but $a = a(q, c) \cup a(q, \phi)$; neither source is sufficient alone, but their combined information yields the final answer.
- Conflicting: $a(q, c) \neq a(q, \phi)$ and $(a = a(q, c)) \oplus (a = a(q, \phi))$; the final answer aligns exclusively with one knowledge source while rejecting the other.
- Irrelevant: $c \perp q$ such that $a(q, c)$ is null or nonsensical; the context c contains no semantic information relevant to the query q . In this case, the model ignores the context entirely and relies solely on PK ($a = a(q, \phi)$) to formulate a response.
- Knowledge Suppression (noise): $a(q, c) = a(q, \phi) \neq a$; both sources agree on an answer, yet the model fails to utilize either, producing an erroneous or unrelated prediction.

This taxonomy enables a systematic investigation of how PK and CK interact throughout NLE generation, moving beyond a binary conflict to capture a spectrum of dynamics. We reformulate this intent-driven answer control and w_b denote the joint intent of w_c and w_p that illustrates the intrinsic model behaviour in generating the final answer a , considering both the PK and CK governed by the underlying interaction scenario. Unlike in Minder et al. (2025), where w_c and w_p are represented using one orthonormal direction in a learned rank-1 projection subspace, we represent w_c and w_p using two orthonormal directions, and $w_b \rightarrow w_c$ and $w_b \rightarrow w_p$ indicate the individual contributions of CK and PK, respectively, in generating a . Then the joint intent $w_b = f(w_c, w_p)$ indicates different knowledge interaction scenarios decided by individual contributions from w_c and w_p . We learn this knowledge interaction function using a rank-2 projection subspace. The prompt template for the three intent-driven answer control is described in Table 1 in

§A.1.2.

3.3. Localize Intent-Guided PK-CK Interactions

In this section, we describe where the intent-guided knowledge interaction emerges in the model space, followed by how the LM encodes it.

Identifying important layers for rank-1 projection subspace. We follow the activation patching-based mechanistic interpretability approach, Patchscope (Minder et al., 2025). They construct two minimally different prompts s and t as ‘source’ and ‘target’, with the same q and c , only differing by the intent, resulting in two different intended answers (following the prompt template in Table 1). To identify the layers capturing the intent present in s , during the forward pass of the target $p(\cdot|t)$, the activation from the hidden state of a particular layer is replaced by the activations from the same layer with the source $p(\cdot|s)$, resulting in $\tilde{p}(\cdot|t) \approx p(\cdot|s)$. Since they only consider the ‘conflicting’ behaviours in understanding the knowledge interaction in LMs, they construct two patching datasets capturing opposite directions: $\mathcal{D}_w^{(c \rightarrow p)} = \{((q, c, w_c), a(q, c)), ((q, c, w_p), a(q, \phi))\}$ for encoding the CK direction, and $\mathcal{D}_w^{(p \rightarrow c)} = \{((q, c, w_p), a(q, \phi)), ((q, c, w_c), a(q, c))\}$ for encoding the PK direction. Layers capturing CK and PK directions, respectively, are selected as:

$$\begin{aligned} \mathbb{L}_{c \rightarrow p} &= \{l \in [1, L] \mid \tilde{p}(a(q, c) \mid q, c, w_p) \geq \tau_c\}, \\ \mathbb{L}_{p \rightarrow c} &= \{l \in [1, L] \mid \tilde{p}(a(q, \phi) \mid q, c, w_c) \geq \tau_p\}, \end{aligned} \quad (2)$$

where τ_c, τ_p are hyperparameters. For more details, please refer to Minder et al. (2025).

Identifying important layers for rank-2 projection subspace (showing the individual knowledge contribution towards generating a , i.e. $w_b \rightarrow w_c$ and $w_b \rightarrow w_p$). We again follow Patchscope and prepare two patching datasets $\mathcal{D}_w^{(b \rightarrow p)} = \{((q, c, w_b), a), ((q, c, w_p), a(q, \phi))\}$ for encoding the contribution of PK interacting with CK in generating a , and $\mathcal{D}_w^{(b \rightarrow c)} = \{((q, c, w_b), a), ((q, c, w_c), a(q, c))\}$ for encoding the contribution of CK interacting with PK in generating a . Important layers $\mathbb{L}_{b \rightarrow c}$ and $\mathbb{L}_{b \rightarrow p}$ are selected using Equation (2) (hyperparameter details are described in Figure 10 in §A.1.3)).

Encoding the intent via rank-1 subspace projection. Once we identify the important layers capturing the behaviour of targeted knowledge interaction, we aim to identify how the LM encodes it. Minder et al. (2025) hypothesize that LMs encode knowledge interaction within their parameter space using a low-rank projection subspace. They model this projection subspace $\mathbf{P} \in \mathbb{R}^{d \times d}$ by a rank-1 unit norm direction $\vec{\mathbf{u}} \in \mathbb{R}^d$ indicating the unidirectional PK-CK conflicting interaction as $\mathbf{P} = \vec{\mathbf{u}}\vec{\mathbf{u}}^T$. At any sequence step

i , the hidden representation $\vec{\mathbf{h}}_i \in \mathbb{R}^d$ for the token e_i in the NLE \mathcal{E} can be linearly decomposed as:

$$\vec{\mathbf{h}}_i = (\mathbf{I} - \mathbf{P})\vec{\mathbf{h}}_i + \mathbf{P}\vec{\mathbf{h}}_i \quad (3)$$

$$= (\mathbf{I} - \mathbf{P})\vec{\mathbf{h}}_i + \vec{\mathbf{u}} \langle \vec{\mathbf{u}}^T, \vec{\mathbf{h}}_i \rangle \quad (4)$$

$(\mathbf{I} - \mathbf{P})$ component of $\vec{\mathbf{h}}_i$ captures other properties in the embedding space, and the $\langle \vec{\mathbf{u}}^T, \vec{\mathbf{h}}_i \rangle$ captures the PK-CK knowledge contribution in the PK-CK conflicting direction $\vec{\mathbf{u}}$. We hypothesize that the rank-1 projection subspace \mathbf{P} can not disentangle the individual knowledge contributions for different knowledge interaction scenarios. We theoretically argue that \mathbf{P} fails to satisfy ‘bijective’ properties of mapping from knowledge direction to individual knowledge contribution for all types of knowledge interaction.

Theorem 3.1 (Non-identifiability under rank-1). *Let the hidden representation $\vec{\mathbf{h}}_i$ for the input x_i at the sequence step i is decomposed as*

$$\vec{\mathbf{h}}_i = c_i \vec{\mathbf{u}}_{CK} + p_i \vec{\mathbf{u}}_{PK} + \xi_i,$$

where $\vec{\mathbf{u}}_{CK}, \vec{\mathbf{u}}_{PK}$ are orthonormal directions corresponding to context and parametric knowledge, $c_i, p_i \in \mathbb{R}$ are their contributions, and ξ_i is noise orthogonal to their span. A rank-1 probe with vector $\vec{\mathbf{v}}$ observes

$$\alpha_i = \vec{\mathbf{v}}^T \vec{\mathbf{h}}_i = c_i \langle \vec{\mathbf{v}}, \vec{\mathbf{u}}_{CK} \rangle + p_i \langle \vec{\mathbf{v}}, \vec{\mathbf{u}}_{PK} \rangle.$$

Then (c_i, p_i) are not uniquely identifiable from α_i whenever both coefficients are nonzero.

Proof. Let $a = \langle \vec{\mathbf{v}}, \vec{\mathbf{u}}_{CK} \rangle$ and $b = \langle \vec{\mathbf{v}}, \vec{\mathbf{u}}_{PK} \rangle$. For any (c, p) , choose $(c', p') = (c + \delta, p - \frac{a}{b}\delta)$ with $\delta \neq 0$. Then $ac + bp = a c' + b p'$, so infinitely many (c', p') yield the same observation. Thus the mapping $(c, p) \mapsto \alpha$ is non-injective, and the individual contributions cannot be disentangled.

Encoding the intent via rank-2 subspace projection.

Once we identify important layers for $w_b \rightarrow w_c$ and $w_b \rightarrow w_p$, we learn the joint intent function f encoding how individual knowledge contributions $w_b \rightarrow w_c$ and $w_b \rightarrow w_p$ are mixed to generate the final answer a using the common layers from $\mathbb{L}_{b \rightarrow c}$ and $\mathbb{L}_{b \rightarrow p}$ via a rank-2 projection subspace \mathbf{P} spanned by two orthogonal directions $\vec{\mathbf{u}} \in \mathbb{R}^{d \times 2}$ as $\mathbf{P} = \vec{\mathbf{u}}(\vec{\mathbf{u}}^T \vec{\mathbf{u}})^{-1} \vec{\mathbf{u}}^T$. Since we aim to identify individual contributions from the individual directions, following Minder et al. (2025), we consider those two basis vectors as orthonormal and hence the rank-2 projection subspace \mathbf{P} is reduced to $\mathbf{P} = \vec{\mathbf{u}}\vec{\mathbf{u}}^T$, since $\vec{\mathbf{u}}^T \vec{\mathbf{u}} = \mathbf{I}_2$. Considering $\vec{\mathbf{u}} = [\vec{\mathbf{u}}_c; \vec{\mathbf{u}}_p]$, at any sequence step i , the hidden representation $\vec{\mathbf{h}}_i \in \mathbb{R}^d$ for the token e_i in the NLE \mathcal{E} can be linearly decomposed as:

$$\vec{\mathbf{h}}_i = (\mathbf{I} - \mathbf{P})\vec{\mathbf{h}}_i + \mathbf{P}\vec{\mathbf{h}}_i \quad (5)$$

$$= (\mathbf{I} - \mathbf{P})\vec{\mathbf{h}}_i + \vec{\mathbf{u}} \langle \vec{\mathbf{u}}^T, \vec{\mathbf{h}}_i \rangle \quad (6)$$

$$= (\mathbf{I} - \mathbf{P})\vec{\mathbf{h}}_i + \vec{\mathbf{u}}_c \langle \vec{\mathbf{u}}_c^T, \vec{\mathbf{h}}_i \rangle + \vec{\mathbf{u}}_p \langle \vec{\mathbf{u}}_p^T, \vec{\mathbf{h}}_i \rangle \quad (7)$$

Learning the rank-2 projection subspace. Let $\tilde{\mathbf{h}}^{w_p} = (\mathbf{I} - \mathbf{P})\tilde{\mathbf{h}} + \tilde{\mathbf{u}}_c \langle \tilde{\mathbf{u}}_c^T, \tilde{\mathbf{h}} \rangle + \tilde{\mathbf{u}}_p \langle \tilde{\mathbf{u}}_p^T, \tilde{\mathbf{h}} \rangle$, and $\tilde{\mathbf{h}}^{w_c} = (\mathbf{I} - \mathbf{P})\tilde{\mathbf{h}} + \tilde{\mathbf{u}}_c \langle \tilde{\mathbf{u}}_c^T, \tilde{\mathbf{h}} \rangle + \tilde{\mathbf{u}}_p \langle \tilde{\mathbf{u}}_p^T, \tilde{\mathbf{h}} \rangle$ be two patched decompositions of the last-token hidden representation of the NLE \mathcal{E} by replacing the activation from a particular layer $l \in \mathbb{L}_{b \rightarrow p} \cup \mathbb{L}_{b \rightarrow c}$ during the forward pass of $p(\cdot \mid q, c, w_b)$ with the activations from the same layer of the forward pass of $p(\cdot \mid q, c, w_p)$ and $p(\cdot \mid q, c, w_c)$, respectively. Then we learn the projection subspace \mathbf{P} spanned by the two orthonormal basis vectors $\tilde{\mathbf{u}} = [\tilde{\mathbf{u}}_c; \tilde{\mathbf{u}}_p]$ by minimizing the two objectives sequentially, maintaining orthonormal directions between $\tilde{\mathbf{u}}_c$ and $\tilde{\mathbf{u}}_p$:

$$\mathcal{J}_p = -\frac{1}{N} \sum_{n=1}^N \log(\tilde{p}(a(q_n, \phi) \mid \tilde{\mathbf{h}}_{(n)}^{w_p})), \quad (8)$$

$$\mathcal{J}_c = -\frac{1}{N} \sum_{n=1}^N \log(\tilde{p}(a(q_n, c_n) \mid \tilde{\mathbf{h}}_{(n)}^{w_c})). \quad (9)$$

Normalized PK-CK score. At any sequence step i , given the hidden representation $\tilde{\mathbf{h}}_i \in \mathbb{R}^d$ for the token e_i in the NLE \mathcal{E} , let $c_i = |\langle \tilde{\mathbf{u}}_c^T, \tilde{\mathbf{h}}_i \rangle|$ and $p_i = |\langle \tilde{\mathbf{u}}_p^T, \tilde{\mathbf{h}}_i \rangle|$, then the normalized contribution from CK and PK can be computed as $\alpha_i^c = c_i / (c_i + p_i)$ and $\alpha_i^p = p_i / (c_i + p_i)$, and $\alpha_i^c, \alpha_i^p \in [0, 1]$ satisfying the identifiability of individual knowledge contribution (Theorem 3.1) under rank-2 subspace. The methodology of assigning the PK-CK direction to the basis vector $\tilde{\mathbf{u}}$ is described in §A.1.1.

4. Results

In this section, we empirically investigate the four research questions proposed in §1.

4.1. Experimental Setting

Dataset and Model: We conduct experiments on three open-weight decoder-only instruct-based LMs: Llama-3.1-8B (Meta-Team, 2024), Gemma-2 9B (Gemma-Team, 2024) and Mistral-v0.3 7B (Jiang et al., 2023) using four publicly available QA datasets: BaseFakepedia, MultihopFakepedia (Minder et al., 2025), StrategyQA (Geva et al., 2021), and OpenBookQA (Mihaylov et al., 2018; Cheng et al., 2024). BaseFakepedia is a knowledge conflict dataset containing queries with 23 relations from Wikipedia. MultihopFakepedia is an extension of BaseFakepedia that contains queries that require extra-hop reasoning to generate answers. Both BaseFakepedia and MultihopFakepedia datasets are utilized for the rank-1 subspace analysis in Minder et al. (2025). StrategyQA is a multi-hop reasoning QA dataset that includes implicit reasoning steps in the queries. OpenBookQA is a commonsense reasoning-based QA dataset. Both StrategyQA and OpenBookQA datasets include ‘supportive’, ‘complementary’, ‘conflicting’, ‘irrelevant’, and ‘knowledge

suppression’ PK-CK interactions, illustrated in Cheng et al. (2024).

Evaluation Metric: To empirically verify the insufficiency of the rank-1 projection subspace in disentangling individual knowledge contributions, we utilize two specific metrics:

Subspace component: For each knowledge interaction type, we compute the subspace component $\langle \tilde{\mathbf{u}}^T, \tilde{\mathbf{h}}_a \rangle$ of the hidden representation of the answer token $\tilde{\mathbf{h}}_a$, which is equivalent to the scalar component of the basis vector $\tilde{\mathbf{u}}$ for the rank-1 projection subspace \mathbf{P} (Minder et al., 2025). If \mathbf{P} adequately captures PK-CK interactions in the dataset, then the distribution of these subspace components should have a mean significantly different from 0. Such a pattern would indicate minimal contribution in the orthogonal complement $(\mathbf{I} - \mathbf{P})$ and reflect distinct, disentangled interaction behavior across different knowledge types.

Explained Variance (Cumulative): Consider the matrix $H = [\{\tilde{\mathbf{h}}_{a_j}\}_{j=1}^N]$, $H \in \mathbb{R}^{N \times d}$ as the concatenation of hidden representation $\tilde{\mathbf{h}}_a \in \mathbb{R}^d$ of the answer token a over N examples. The d singular values $\sigma_1 \gg \sigma_2, \dots \gg \sigma_d$ from the diagonal matrix $\Sigma \in \mathbb{R}^{d \times d}$ after the Singular Value Decomposition (SVD) of $HH^T = A\Sigma B$ indicates the strength of HH^T in d orthonormal directions. For top- r singular values $\sigma_1 \gg \sigma_2, \dots \gg \sigma_r$, the cumulative explained variance EV_r : $EV_r = \frac{\sum_{j=1}^r \sigma_j^2}{\sum_{j=1}^d \sigma_j^2}$

indicates the sufficiency of rank- r projection subspace in encoding the variance in knowledge interactions present in the dataset (Wall et al., 2003; Lazzaretto et al., 2025). If the rank-1 projection subspace \mathbf{P} adequately captures PK-CK interactions in the dataset, then the cumulative explained variance at rank-1 EV_1 should approximate 1.0.

4.2. RQ1: Is a Rank-1 Projection Subspace Enough for Disentangling PK and CK Contribution in All Types of Knowledge Interaction Scenarios?

Figure 2 shows, for each dataset, the distribution of the rank-1 subspace component $\langle \tilde{\mathbf{u}}^T, \tilde{\mathbf{h}}_a \rangle$, where $\tilde{\mathbf{h}}_a$ is the hidden state of the answer token and $\tilde{\mathbf{u}}$ is the learned rank-1 interaction direction. Each colored curve corresponds to one knowledge interaction type and shows how strongly answer representations align with $\tilde{\mathbf{u}}$ (x-axis); the y-axis denotes the relative frequency, estimated via kernel density smoothing.

Across all datasets and knowledge interaction types (§3.2), the mean of the subspace component distribution converges to 0, indicating significant contribution from the orthogonal complement $(\mathbf{I} - \mathbf{P})$, showing insufficiency of the rank-1 projection subspace \mathbf{P} in encoding the PK-CK interaction. This observed behaviour for the ‘complementary’ and ‘supportive’ interactions supports our hypothesis that, for examples where both PK and CK contribute equally, the rank-1 \mathbf{P}

fails to distinctly encode individual contributions. However, surprisingly, we observe a similar behaviour for the ‘conflicting’ interaction type as well, illustrating that \mathbf{P} fails to also differentiate where the conflicts arise from. We observe similar results for the other two models (see Section A.2). These results indicate that *different knowledge interactions are poorly captured by the rank-1 projection subspace*, with most of the interaction signal residing in the orthogonal complement ($\mathbf{I} - \mathbf{P}$), thereby suggesting the *necessity of a higher-rank subspace to effectively disentangle PK-CK contributions*.

To understand the minimum rank required for the learnt projection subspace where the orthogonal complement contribution is minimum and it encodes different knowledge interaction types, we plot the cumulative explained variance EV_r for different ranks across all datasets and models in Figure 3. EV_r reaches 1.0 at rank-2 and converges thereafter for all datasets and models.

4.3. RQ2: How Do Individual PK and CK Contributions Change Over the NLE Generation for Different Knowledge Interactions?

In this section, we investigate the dynamics of individual PK and CK contribution α_i^p and α_i^c at every sequence step i over the NLE \mathcal{E} generation. Among the four datasets, OpenBookQA shows the largest jump in cumulative explained variance from rank-1 to rank-2 across all models (Figure 3). We therefore use OpenBookQA as our development set to (i) locate intent-sensitive layers via activation patching and (ii) learn the rank-2 projection subspace. We then freeze these choices and evaluate the resulting rank-2 subspace on all datasets. We also utilize the StrategyQA dataset and found that the learned parametric and contextual directions are highly stable, with average directional similarity exceeding 0.9 for both axes (§A.3). We begin by identifying important layers for encoding individual knowledge contributions to generate the final answer in the rank-2 projection subspace. Figure 4 shows that patching from $w_b \rightarrow w_p$ (BOTH→PRI) (L13–18) yields a larger probability gain than $w_b \rightarrow w_c$ (BOTH→CTX) (L15–17), indicating that Llama-3.1-8B-Instruct relies more on PK than on CK for OpenBookQA. We observe similar results for gemma-2-9b-it and Mistral-7B-Instruct-v0.3 (see Figures 13 and 14). This PK dominance in a context-rich task suggests that the model tends to recall commonsense information from memory rather than grounding answers in the provided context, highlighting potential for future work on context-sensitive knowledge control.

To identify the individual knowledge contribution in generating the final answer token a , we project its hidden representation \mathbf{h}_a to the rank-2 projection subspace to compute the α_i^p and α_i^c as the PK-CK contributions. Figure 5a indicates

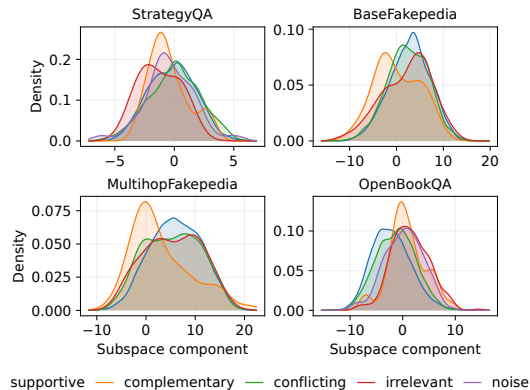


Figure 2. Kernel Density Estimate (KDE) of the PK-CK subspace component $\langle \vec{u}^T, \vec{h}_i \rangle$ across different knowledge interaction types for four QA datasets using Mistral-7B-Instruct-v0.3.

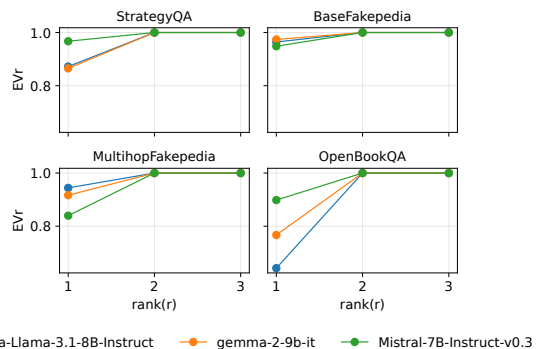


Figure 3. Cumulative explained variance (EV_r) at rank(r) from the three models using the four QA datasets. At rank-2, it reaches 1.0 value, indicating sufficiency in capturing different knowledge interaction variants.

an overall higher CK contribution for the BaseFakepedia and MultihopFakepedia, and a higher PK contribution for the StrategyQA and OpenBookQA for the Meta-Llama-3.1-8B-Instruct model. This is consistent with dataset designs: Fakepedia variants are evidence-centric and often adversarial/conflicting, pushing the model to prefer the provided context; StrategyQA/OpenBookQA rely more on commonsense priors and sparse cues, which encourage parametric recall. To understand the reason behind this knowledge interaction behaviour for these datasets, we investigate the distribution of different knowledge interactions in Fig. 5b. We find that both BaseFakepedia and MultihopFakepedia contain more conflicting examples than other knowledge interaction types (as defined in §3.2). Prior works (Cheng et al., 2024; Tao et al., 2024) suggest that for ‘conflicting’ examples, models tend to suppress PK when sufficient and relevant information is present in CK and for ‘supporting’ examples, models rely more on PK, with CK acting as a regularizer. Also, Tao et al. (2024) suggests that parametric recall is the default unless explicitly overridden by con-

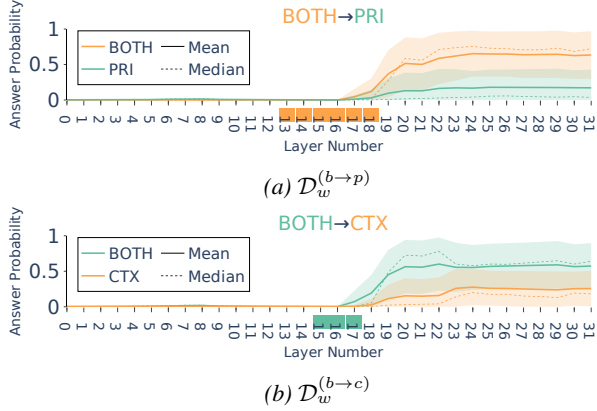


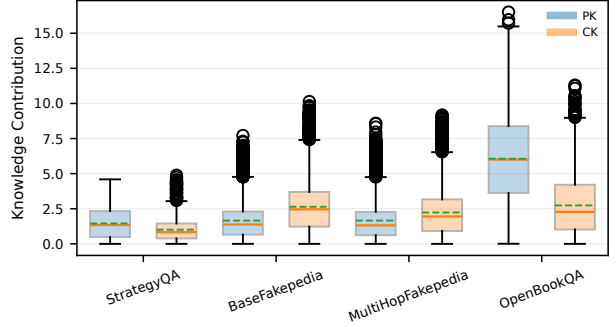
Figure 4. Patchscope on OpenBookQA from Meta-Llama-3.1-8B-Instruct. (a) Activation patching on $\mathcal{D}_w^{(b \rightarrow p)}$. (b) Activation patching on $\mathcal{D}_w^{(b \rightarrow c)}$.

text. Overall, we conclude that *for conflicting examples, the model aligns more with the CK direction and for supportive examples, the model aligns more with the PK direction in the rank-2 projection subspace*, supporting observations from prior works.

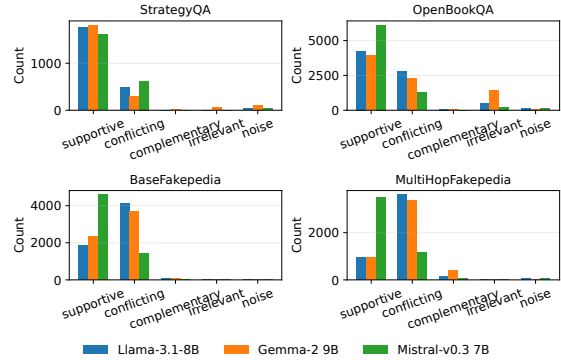
To understand the knowledge interaction dynamics during NLE generation (prompt template is described in Tab. 9 in §A.1.2), we analyze variation in α_i^p and α_i^c over all sequence steps of NLE generation for different knowledge interaction scenarios. Figure 6 shows that for all datasets, *during most of the NLE generations, the model starts with a higher CK, then considers both PK and CK with slight prioritization of PK*. However, for longer NLEs, CK and PK compete with each other with higher fluctuation. Longer NLEs indicate difficult examples with higher depth in multi-hop reasoning and higher token uncertainty (from Figure 16), which force the model to iteratively reconcile PK with CK, resulting in this fluctuating behavior.

4.4. RQ3: Can We Find Reasons for Hallucinations Based on PK-CK Interactions?

To characterize the knowledge interaction dynamics during the NLE generation in terms of context faithfulness, we investigate the knowledge alignments of hallucinated vs non-hallucinated responses in the rank-2 projection subspace. We utilize two RAG hallucination datasets: RAGTruth and Dollo (AC) (Sun et al., 2025), of sizes 18240 and 297 examples respectively, containing examples from QA, Summarisation and Information Extraction. Each dataset provides human-annotated spans indicating hallucinated content across responses from multiple models. Importantly, whether a span is labelled as hallucinated is *model-dependent*: the same RAG input may yield hallucinated text for one model but not for another. Due to the limited number of models covered in the two datasets, we consider only the



(a) Individual PK-CK contribution in generating the answer token.



(b) Distribution of knowledge interaction types across datasets.

Figure 5. Answer-level PK-CK alignment and distribution of knowledge interaction types across datasets.

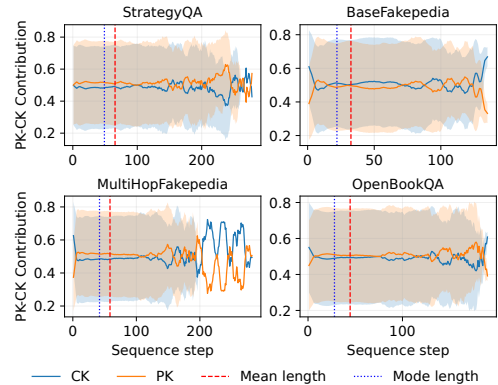


Figure 6. PK-CK interaction dynamics over the sequence steps for Meta-Llama-3.1-8B-Instruct. The dotted red and blue lines indicate the mean and mode of NLE lengths. Figure 15 contains PK-CK dynamics for different interaction scenarios.

data split corresponding to the Meta-Llama-3.1-8B-Instruct model. Fig. 7 illustrates the PK-CK knowledge interaction dynamics. The gap between PK and CK is much higher for the examples with hallucinated spans than for the examples with no hallucinated spans across the sequence steps. This result also aligns with similar observations of *positive correlation of PK and hallucination* in Sun et al. (2025).

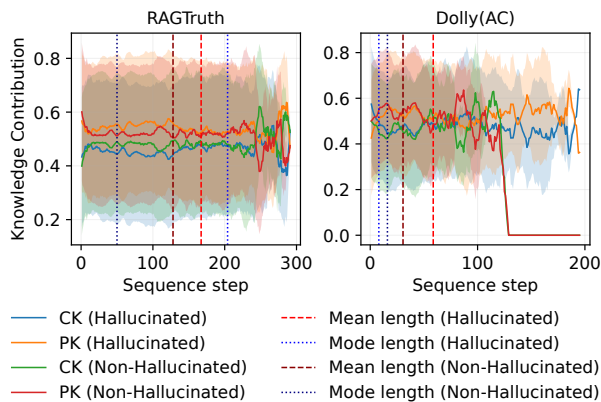


Figure 7. PK-CK interaction dynamics over the sequence step from Meta-Llama-3.1-8B-Instruct for the two RAG hallucination datasets.

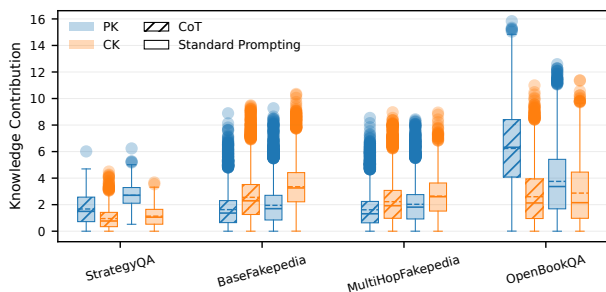


Figure 8. Comparison in individual PK-CK contribution in generating the answer token a for all the datasets from Meta-Llama-3.1-8B-Instruct model between CoT and standard prompting.

4.5. RQ4: How is the CoT mechanism aligned with the knowledge interaction subspace?

To verify whether reasoning-based prompting CoT helps the model to stay aligned with the CK and reduces reliance on PK, we compare the PK-CK contribution in generating the final answer between standard prompting and CoT prompting (prompt template is described in Tab. 9 in §A.1.2). Fig. 8 indicates that *CoT maintains similar CK alignment compared to standard prompting for all the datasets, and also reduces PK alignment except for the OpenBookQA dataset.*

5. Discussion

PK-CK interaction is multidimensional, not binary. Our results provide a new insight into how Large Language Models (LLMs) integrate Parametric Knowledge (PK) and Context Knowledge (CK) when generating Natural Language Explanations (NLEs). Prior work typically treats PK-CK interaction as a one-dimensional phenomenon (Longpre et al., 2021; Minder et al., 2025; Xu et al., 2024), assuming that models “choose” between relying on either internal parameters or external context. In contrast, our findings demon-

strate that this interaction is inherently multidimensional. Our proposed rank-2 projection subspace captures not only conflicts but also complementary and supportive PK-CK relations, revealing that NLE generation also involves dynamic coordination rather than competition between the two knowledge sources.

Rank-2 subspace enables identifiable PK and CK contributions. The inadequacy of the rank-1 representation highlights that prior linear or scalar formulations collapse distinct interaction types, leading to inaccurate interpretations of knowledge interactions. By separating PK and CK directions, our framework enables identifiable tracking of their complementary individual contributions across sequence steps. This provides a geometric perspective on how models negotiate between internal recall and contextual grounding throughout reasoning, establishing a mechanistic basis for assessing context-faithfulness of NLE.

Causal Alignment of Hallucination with PK and CoT with CK in the Rank-2 Subspace. Empirically, the strong alignment of sequences with hallucinated spans with the PK direction extends causal findings from Sun et al. (2025), suggesting that *hallucination reflects a systematic bias toward parametric recall rather than random generation noise.* Conversely, faithful and contextually grounded NLEs balance contributions from both knowledge axes, indicating that equilibrium in the learned subspace corresponds to factual reliability. Similarly, our analysis of CoT prompting shows that CoT operates as a distinct low-rank subspace aligned more with CK, clarifying why it enhances contextual grounding without fully suppressing PK influence (Tao et al., 2025).

6. Conclusion

This work shows that the interaction between Parametric Knowledge (PK) and Context Knowledge (CK) in LLMs is inherently multidimensional rather than a binary choice. We introduce a rank-2 projection framework that (i) resolves the non-identifiability of rank-1 probes, (ii) disentangles token-level PK and CK components, and (iii) enables the first systematic multi-step analysis of PK-CK dynamics during Natural Language Explanation (NLE) generation. Across four QA datasets and three open-weight instruction-tuned LMs, rank-1 subspaces fail to capture diverse interaction regimes, whereas rank-2 suffices to explain the observed variance. Our step-wise analysis further reveals consistent patterns: hallucinated generations align strongly with the PK axis, while context-faithful generations maintain a more balanced PK-CK alignment, and Chain-of-Thought prompting shifts generations toward CK by reducing PK reliance. Beyond NLE generation, this subspace-based analysis provides a general, model-internal signal for studying how LLMs balance internal recall and external grounding.

Acknowledgements

 This research was co-funded by the European Union (ERC, ExplainYourself, 101077481) and by the VIL-LUM FONDEN (grant number 40543). Views and opinions expressed are however those of the author(s) only and do not necessarily reflect those of the European Union or the European Research Council. Neither the European Union nor the granting authority can be held responsible for them.

References

- Atanasova, P., Simonsen, J. G., Lioma, C., and Augenstein, I. Generating Fact Checking Explanations. In Jurafsky, D., Chai, J., Schluter, N., and Tetreault, J. (eds.), *Proceedings of the 58th Annual Meeting of the Association for Computational Linguistics*, pp. 7352–7364, Online, July 2020. Association for Computational Linguistics. doi: 10.18653/v1/2020.acl-main.656. URL <https://aclanthology.org/2020.acl-main.656/>.
- Atanasova, P., Camburu, O.-M., Lioma, C., Lukasiewicz, T., Simonsen, J. G., and Augenstein, I. Faithfulness Tests for Natural Language Explanations. In Rogers, A., Boyd-Graber, J., and Okazaki, N. (eds.), *Proceedings of the 61st Annual Meeting of the Association for Computational Linguistics (Volume 2: Short Papers)*, pp. 283–294, Toronto, Canada, July 2023. Association for Computational Linguistics. doi: 10.18653/v1/2023.acl-short.25. URL <https://aclanthology.org/2023.acl-short.25/>.
- Bi, B., Liu, S., Wang, Y., Xu, Y., Fang, J., Mei, L., and Cheng, X. Parameters vs. Context: Fine-Grained Control of Knowledge Reliance in Language Models, 2025. URL <https://arxiv.org/abs/2503.15888>.
- Brown, T., Mann, B., Ryder, N., Subbiah, M., Kaplan, J. D., Dhariwal, P., Neelakantan, A., Shyam, P., Sastry, G., Askell, A., Agarwal, S., Herbert-Voss, A., Krueger, G., Henighan, T., Child, R., Ramesh, A., Ziegler, D., Wu, J., Winter, C., Hesse, C., Chen, M., Sigler, E., Litwin, M., Gray, S., Chess, B., Clark, J., Berner, C., McCandlish, S., Radford, A., Sutskever, I., and Amodei, D. Language Models are Few-Shot Learners. In Larochelle, H., Ranzato, M., Hadsell, R., Balcan, M., and Lin, H. (eds.), *Advances in Neural Information Processing Systems*, volume 33, pp. 1877–1901. Curran Associates, Inc., 2020. URL https://proceedings.neurips.cc/paper_files/paper/2020/file/1457c0d6bfc4967418bfb8ac142f64a-Paper.pdf.
- Camburu, O.-M., Rocktäschel, T., Lukasiewicz, T., and Blunsom, P. e-SNLI: Natural Language Inference with Natural Language Explanations. In Bengio, S., Wallach, H., Larochelle, H., Grauman, K., Cesa-Bianchi, N., and Garnett, R. (eds.), *Advances in Neural Information Processing Systems*, volume 31. Curran Associates, Inc., 2018. URL https://proceedings.neurips.cc/paper_files/paper/2018/file/4c7a167bb329bd92580a99ce422d6fa6-Paper.pdf.
- Cheng, S., Pan, L., Yin, X., Wang, X., and Wang, W. Y. Understanding the Interplay between Parametric and Contextual Knowledge for Large Language Models, 2024. URL <https://arxiv.org/abs/2410.08414>.
- Clark, K., Khandelwal, U., Levy, O., and Manning, C. D. What Does BERT Look at? An Analysis of BERT’s Attention. In Linzen, T., Chrupała, G., Belinkov, Y., and Hupkes, D. (eds.), *Proceedings of the 2019 ACL Workshop BlackboxNLP: Analyzing and Interpreting Neural Networks for NLP*, pp. 276–286, Florence, Italy, August 2019. Association for Computational Linguistics. doi: 10.18653/v1/W19-4828. URL <https://aclanthology.org/W19-4828/>.
- Elhage, N., Hume, T., Olsson, C., Schiefer, N., Henighan, T., Kravec, S., Hatfield-Dodds, Z., Lasenby, R., Drain, D., Chen, C., Grosse, R., McCandlish, S., Kaplan, J., Amodei, D., Wattenberg, M., and Olah, C. Toy Models of Superposition. *Transformer Circuits Thread*, 2022. URL https://transformer-circuits.pub/2022/toy_model/index.html.
- Gemma-Team. Gemma 2: Improving Open Language Models at a Practical Size, 2024. URL <https://arxiv.org/abs/2408.00118>.
- Geva, M., Khashabi, D., Segal, E., Khot, T., Roth, D., and Berant, J. Did Aristotle Use a Laptop? A Question Answering Benchmark with Implicit Reasoning Strategies. *Transactions of the Association for Computational Linguistics*, 9:346–361, 04 2021. ISSN 2307-387X. doi: 10.1162/tacl.a.00370. URL <https://doi.org/10.1162/tacl.a.00370>.
- Hagström, L., Marjanovic, S. V., Yu, H., Arora, A., Lioma, C., Maistro, M., Atanasova, P., and Augenstein, I. A reality check on context utilisation for retrieval-augmented generation. In Che, W., Nabende, J., Shutova, E., and Pilehvar, M. T. (eds.), *Proceedings of the 63rd Annual Meeting of the Association for Computational Linguistics (Volume 1: Long Papers)*, pp. 19691–19730, Vienna, Austria, July 2025. Association for Computational Linguistics. ISBN 979-8-89176-251-0. doi: 10.18653/v1/2025.acl-long.968. URL <https://aclanthology.org/2025.acl-long.968/>.
- Hewitt, J. and Manning, C. D. A Structural Probe for Finding Syntax in Word Representations. In Burstein, J.,

- Doran, C., and Solorio, T. (eds.), *Proceedings of the 2019 Conference of the North American Chapter of the Association for Computational Linguistics: Human Language Technologies, Volume 1 (Long and Short Papers)*, pp. 4129–4138, Minneapolis, Minnesota, June 2019. Association for Computational Linguistics. doi: 10.18653/v1/N19-1419. URL <https://aclanthology.org/N19-1419/>.
- Jiang, A. Q., Sablayrolles, A., Mensch, A., Bamford, C., Chaplot, D. S., de las Casas, D., Bressand, F., Lengyel, G., Lample, G., Saulnier, L., Lavaud, L. R., Lachaux, M.-A., Stock, P., Scao, T. L., Lavril, T., Wang, T., Lacroix, T., and Sayed, W. E. Mistral 7B, 2023. URL <https://arxiv.org/abs/2310.06825>.
- Jiang, Z., Xu, F. F., Araki, J., and Neubig, G. How Can We Know What Language Models Know? *Transactions of the Association for Computational Linguistics*, 8:423–438, 2020. doi: 10.1162/tacl.a.00324. URL <https://aclanthology.org/2020.tacl-1.28/>.
- Lampinen, A., Dasgupta, I., Chan, S., Mathewson, K., Tessler, M., Creswell, A., McClelland, J., Wang, J., and Hill, F. Can language models learn from explanations in context? In Goldberg, Y., Kozareva, Z., and Zhang, Y. (eds.), *Findings of the Association for Computational Linguistics: EMNLP 2022*, pp. 537–563, Abu Dhabi, United Arab Emirates, December 2022. Association for Computational Linguistics. doi: 10.18653/v1/2022.findings-emnlp.38. URL <https://aclanthology.org/2022.findings-emnlp.38/>.
- Lazzaretto, M., Peters, J., and Pfister, N. Invariant subspace decomposition. *Journal of Machine Learning Research*, 26(95):1–56, 2025. URL <http://jmlr.org/papers/v26/24-0699.html>.
- Longpre, S., Perisetla, K., Chen, A., Ramesh, N., DuBois, C., and Singh, S. Entity-Based Knowledge Conflicts in Question Answering. In Moens, M.-F., Huang, X., Specia, L., and Yih, S. W.-t. (eds.), *Proceedings of the 2021 Conference on Empirical Methods in Natural Language Processing*, pp. 7052–7063, Online and Punta Cana, Dominican Republic, November 2021. Association for Computational Linguistics. doi: 10.18653/v1/2021.emnlp-main.565. URL <https://aclanthology.org/2021.emnlp-main.565/>.
- Marjanovic, S. V., Yu, H., Atanasova, P., Maistro, M., Lioma, C., and Augenstein, I. DYNAMICQA: Tracing internal knowledge conflicts in language models. In Al-Onaizan, Y., Bansal, M., and Chen, Y.-N. (eds.), *Findings of the Association for Computational Linguistics: EMNLP 2024*, pp. 14346–14360, Miami, Florida, USA, November 2024. Association for Computational Linguistics. doi: 10.18653/v1/2024.findings-emnlp.838. URL <https://aclanthology.org/2024.findings-emnlp.838/>.
- Meta-Team. The Llama 3 Herd of Models, 2024. URL <https://arxiv.org/abs/2407.21783>.
- Mihaylov, T., Clark, P., Khot, T., and Sabharwal, A. Can a Suit of Armor Conduct Electricity? A New Dataset for Open Book Question Answering. In Riloff, E., Chiang, D., Hockenmaier, J., and Tsujii, J. (eds.), *Proceedings of the 2018 Conference on Empirical Methods in Natural Language Processing*, pp. 2381–2391, Brussels, Belgium, October–November 2018. Association for Computational Linguistics. doi: 10.18653/v1/D18-1260. URL <https://aclanthology.org/D18-1260/>.
- Minder, J., Du, K., Stoehr, N., Monea, G., Wendler, C., West, R., and Cotterell, R. Controllable Context Sensitivity and the Knob Behind It. In *The Thirteenth International Conference on Learning Representations*, 2025. URL <https://openreview.net/forum?id=Igm9bbkzHC>.
- Petroni, F., Rocktäschel, T., Riedel, S., Lewis, P., Bakhtin, A., Wu, Y., and Miller, A. Language Models as Knowledge Bases? In Inui, K., Jiang, J., Ng, V., and Wan, X. (eds.), *Proceedings of the 2019 Conference on Empirical Methods in Natural Language Processing and the 9th International Joint Conference on Natural Language Processing (EMNLP-IJCNLP)*, pp. 2463–2473, Hong Kong, China, November 2019. Association for Computational Linguistics. doi: 10.18653/v1/D19-1250. URL <https://aclanthology.org/D19-1250/>.
- Rajani, N. F., McCann, B., Xiong, C., and Socher, R. Explain Yourself! Leveraging Language Models for Commonsense Reasoning. In Korhonen, A., Traum, D., and Márquez, L. (eds.), *Proceedings of the 57th Annual Meeting of the Association for Computational Linguistics*, pp. 4932–4942, Florence, Italy, July 2019. Association for Computational Linguistics. doi: 10.18653/v1/P19-1487. URL <https://aclanthology.org/P19-1487/>.
- Roberts, A., Raffel, C., and Shazeer, N. How Much Knowledge Can You Pack Into the Parameters of a Language Model? In Webber, B., Cohn, T., He, Y., and Liu, Y. (eds.), *Proceedings of the 2020 Conference on Empirical Methods in Natural Language Processing (EMNLP)*, pp. 5418–5426, Online, November 2020. Association for Computational Linguistics. doi: 10.18653/v1/2020.emnlp-main.437. URL <https://aclanthology.org/2020.emnlp-main.437/>.
- Siegel, N., Camburu, O.-M., Heess, N., and Perez-Ortiz, M. The probabilities also matter: A more faithful met-

- ric for faithfulness of free-text explanations in large language models. In Ku, L.-W., Martins, A., and Sriku-
mar, V. (eds.), *Proceedings of the 62nd Annual Meeting of the Association for Computational Linguistics (Volume 2: Short Papers)*, pp. 530–546, Bangkok, Thailand, August 2024. Association for Computational Linguistics. doi: 10.18653/v1/2024.acl-short.49. URL <https://aclanthology.org/2024.acl-short.49/>.
- Su, X., Le, T., Bethard, S., and Howard, P. Semi-Structured Chain-of-Thought: Integrating Multiple Sources of Knowledge for Improved Language Model Reasoning. In Duh, K., Gomez, H., and Bethard, S. (eds.), *Proceedings of the 2024 Conference of the North American Chapter of the Association for Computational Linguistics: Human Language Technologies (Volume 1: Long Papers)*, pp. 8597–8613, Mexico City, Mexico, June 2024. Association for Computational Linguistics. doi: 10.18653/v1/2024.naacl-long.475. URL <https://aclanthology.org/2024.naacl-long.475/>.
- Sun, Z., Zang, X., Zheng, K., Xu, J., Zhang, X., Yu, W., Song, Y., and Li, H. ReDeEP: Detecting Hallucination in Retrieval-Augmented Generation via Mechanistic Interpretability. In *The Thirteenth International Conference on Learning Representations*, 2025. URL <https://openreview.net/forum?id=ztzZDzgrh>.
- Tan, X., Zou, B., and Aw, A. T. Improving Explainable Fact-Checking with Claim-Evidence Correlations. In Rambow, O., Wanner, L., Apidianaki, M., Al-Khalifa, H., Eugenio, B. D., and Schockaert, S. (eds.), *Proceedings of the 31st International Conference on Computational Linguistics*, pp. 1600–1612, Abu Dhabi, UAE, January 2025. Association for Computational Linguistics. URL <https://aclanthology.org/2025.coling-main.108/>.
- Tao, Y., Hiatt, A., Haake, E., Jetter, A. J., and Agrawal, A. When Context Leads but Parametric Memory Follows in Large Language Models. In Al-Onaizan, Y., Bansal, M., and Chen, Y.-N. (eds.), *Proceedings of the 2024 Conference on Empirical Methods in Natural Language Processing*, pp. 4034–4058, Miami, Florida, USA, November 2024. Association for Computational Linguistics. doi: 10.18653/v1/2024.emnlp-main.234. URL <https://aclanthology.org/2024.emnlp-main.234/>.
- Tao, Y., Hiatt, A., Seetharaman, R., and Agrawal, A. Lost-in-the-Later?: Framework for Quantifying Contextual Grounding in Large Language Models, 2025. URL <https://arxiv.org/abs/2507.05424>.
- Tenney, I., Das, D., and Pavlick, E. BERT Rediscovered the Classical NLP Pipeline. In Korhonen, A., Traum, D., and Márquez, L. (eds.), *Proceedings of the 57th Annual Meeting of the Association for Computational Linguistics*, pp. 4593–4601, Florence, Italy, July 2019. Association for Computational Linguistics. doi: 10.18653/v1/P19-1452. URL <https://aclanthology.org/P19-1452/>.
- Turpin, M., Michael, J., Perez, E., and Bowman, S. R. Language Models Don’t Always Say What They Think: Unfaithful Explanations in Chain-of-Thought Prompting. In *Thirty-seventh Conference on Neural Information Processing Systems*, 2023. URL <https://openreview.net/forum?id=bzs4uPLXvi>.
- Wall, M. E., Rechtsteiner, A., and Rocha, L. M. *Singular Value Decomposition and Principal Component Analysis*, pp. 91–109. Springer US, Boston, MA, 2003. ISBN 978-0-306-47815-4. doi: 10.1007/0-306-47815-3_5. URL https://doi.org/10.1007/0-306-47815-3_5.
- Wang, H. and Shu, K. Explainable Claim Verification via Knowledge-Grounded Reasoning with Large Language Models. In Bouamor, H., Pino, J., and Bali, K. (eds.), *Findings of the Association for Computational Linguistics: EMNLP 2023*, pp. 6288–6304, Singapore, December 2023. Association for Computational Linguistics. doi: 10.18653/v1/2023.findings-emnlp.416. URL <https://aclanthology.org/2023.findings-emnlp.416/>.
- Wang, Y. and Atanasova, P. ”Self-Critique and Refinement for Faithful Natural Language Explanations”. In Christodoulopoulos, C., Chakraborty, T., Rose, C., and Peng, V. (eds.), *Proceedings of the 2025 Conference on Empirical Methods in Natural Language Processing*, pp. 8481–8507, Suzhou, China, November 2025. Association for Computational Linguistics. ISBN 979-8-89176-332-6. doi: 10.18653/v1/2025.emnlp-main.427. URL <https://aclanthology.org/2025.emnlp-main.427/>.
- Wang, Y., Wang, H., Bai, Y., and Luo, M. Continuously steering LLMs sensitivity to contextual knowledge with proxy models. In Christodoulopoulos, C., Chakraborty, T., Rose, C., and Peng, V. (eds.), *Proceedings of the 2025 Conference on Empirical Methods in Natural Language Processing*, pp. 4682–4698, Suzhou, China, November 2025. Association for Computational Linguistics. ISBN 979-8-89176-332-6. doi: 10.18653/v1/2025.emnlp-main.233. URL <https://aclanthology.org/2025.emnlp-main.233/>.
- Wei, J., Wang, X., Schuurmans, D., Bosma, M., brian ichter, Xia, F., Chi, E. H., Le, Q. V., and Zhou, D. Chain of thought prompting elicits reasoning in large language

- models. In Oh, A. H., Agarwal, A., Belgrave, D., and Cho, K. (eds.), *Advances in Neural Information Processing Systems*, 2022. URL https://openreview.net/forum?id=_VjQlMeSB_J.
- Xu, R., Qi, Z., Guo, Z., Wang, C., Wang, H., Zhang, Y., and Xu, W. Knowledge Conflicts for LLMs: A Survey. In Al-Onaizan, Y., Bansal, M., and Chen, Y.-N. (eds.), *Proceedings of the 2024 Conference on Empirical Methods in Natural Language Processing*, pp. 8541–8565, Miami, Florida, USA, November 2024. Association for Computational Linguistics. doi: 10.18653/v1/2024.emnlp-main.486. URL <https://aclanthology.org/2024.emnlp-main.486/>.
- Yu, H., Atanasova, P., and Augenstein, I. Revealing the parametric knowledge of language models: A unified framework for attribution methods. In Ku, L.-W., Martins, A., and Srikumar, V. (eds.), *Proceedings of the 62nd Annual Meeting of the Association for Computational Linguistics (Volume 1: Long Papers)*, pp. 8173–8186, Bangkok, Thailand, August 2024. Association for Computational Linguistics. doi: 10.18653/v1/2024.acl-long.444. URL <https://aclanthology.org/2024.acl-long.444/>.
- Yuan, S., Sun, J., Zhang, R., Färber, M., Eger, S., Atanasova, P., and Augenstein, I. Graph-guided textual explanation generation framework. In Christodoulopoulos, C., Chakraborty, T., Rose, C., and Peng, V. (eds.), *Proceedings of the 2025 Conference on Empirical Methods in Natural Language Processing*, pp. 29362–29386, Suzhou, China, November 2025a. Association for Computational Linguistics. ISBN 979-8-89176-332-6. doi: 10.18653/v1/2025.emnlp-main.1494. URL <https://aclanthology.org/2025.emnlp-main.1494/>.
- Yuan, X., Yang, Z., Huang, Z., Wang, Y., Fan, S., Ju, Y., Zhao, J., and Liu, K. Exploiting Contextual Knowledge in LLMs through \mathcal{V} -usable Information based Layer Enhancement. In Che, W., Nabende, J., Shutova, E., and Pilehvar, M. T. (eds.), *Proceedings of the 63rd Annual Meeting of the Association for Computational Linguistics (Volume 1: Long Papers)*, pp. 31726–31741, Vienna, Austria, July 2025b. Association for Computational Linguistics. ISBN 979-8-89176-251-0. doi: 10.18653/v1/2025.acl-long.1531. URL <https://aclanthology.org/2025.acl-long.1531/>.
- Zhang, H., Zhang, Y., Li, X., Shi, W., Xu, H., Liu, H., Wang, Y., Shang, L., Liu, Q., Liu, Y., and Tang, R. Evaluating the External and Parametric Knowledge Fusion of Large Language Models, 2024. URL <https://arxiv.org/abs/2405.19010>.
- Zhao, Z., Monti, E., Lehmann, J., and Assem, H. Enhancing Contextual Understanding in Large Language Models through Contrastive Decoding. In Duh, K., Gomez, H., and Bethard, S. (eds.), *Proceedings of the 2024 Conference of the North American Chapter of the Association for Computational Linguistics: Human Language Technologies (Volume 1: Long Papers)*, pp. 4225–4237, Mexico City, Mexico, June 2024. Association for Computational Linguistics. doi: 10.18653/v1/2024.naacl-long.237. URL <https://aclanthology.org/2024.naacl-long.237/>.

A. Appendix

A.1. Replication Details

A.1.1. DETERMINING PK AND CK DIRECTIONS IN THE RANK-2 PROJECTION SUBSPACE.

Once we obtain the rank-2 projection subspace \mathbf{P} spanned by the orthonormal basis vectors $\bar{\mathbf{u}} \in \mathbb{R}^{d \times 2}$, we identify the PK and CK directions as follows:

$$\bar{\mathbf{u}}_p = \arg \max_{\bar{\mathbf{u}}} (\bar{\mathbf{u}}^\top \mathbf{H}_{w_p}), \quad (10)$$

$$\bar{\mathbf{u}}_c = \arg \max_{\bar{\mathbf{u}}} (\bar{\mathbf{u}}^\top \mathbf{H}_{w_c}), \quad (11)$$

where $\mathbf{H}_{w_p} \in \mathbb{R}^{n \times d}$, and $\mathbf{H}_{w_c} \in \mathbb{R}^{n \times d}$ are matrices of hidden representation of answer tokens $a(q, \phi)$ and $a(q, c)$ guided by intents w_p and w_c respectively over n examples.

A.1.2. PROMPT TEMPLATE

Prompt template to generate controlled answers $a(q, \phi)$, $a(q, c)$ and a driven by intents w_p , w_c , and w_b are described in Table 1. The prompt template for generating NLEs and CoT-based prompting over the datasets and models is described in Figure 9.

A.1.3. HYPERPARAMETERS

We identify important layers $\mathbb{L}_{b \rightarrow c}$ and $\mathbb{L}_{b \rightarrow p}$ to capture individual PK and CK contributions, respectively, from the final answer a via Patchscope using the hyperparameters described in Figure 10.

A.2. Additional Results

A.3. Robustness Analysis

We evaluate the robustness of PatchScope localization and the learned rank-2 PK–CK projection subspace along four axes: layer sensitivity, prompt perturbations, context variation, and geometric stability.

PatchScope layer sensitivity. To ensure that PK–CK disentanglement is not tied to a single layer, we evaluate the rank-2 subspace across six PatchScope-identified layers of Meta-Llama-3.1-8B-Instruct (L13–L18). Patching accuracy is stable across 6 layers L13-18, [0.82, 0.84, 0.83, 0.85, 0.87, 0.86], with a mean of 0.84 ± 0.018 and peak performance at L17 (0.87). The resulting stability score of 0.98 indicates that disentanglement consistently emerges across this mid-to-late layer block rather than being a layer-specific artifact.

Prompt perturbation robustness. We test invariance to surface-form variations via paraphrasing, synonym substitution, and word-order perturbations. End-to-end prediction agreement remains high (model-dependent), at 0.92, 0.88, and 0.85 for paraphrase, synonym, and word-order changes, respectively. To assess geometric robustness, we independently learn projection subspaces from original and perturbed prompts and measure their cosine similarity, obtaining mean consistency scores of 0.95 ± 0.04 , 0.93 ± 0.05 , and 0.89 ± 0.08 . These results indicate that the learned subspace is largely insensitive to superficial prompt variations and primarily reflects semantic knowledge alignment.

Context variation sanity check. If the projection subspace captures genuine knowledge interaction, PK-CK contributions should shift with context availability. Varying context from minimal (no context) to medium (first 50 CK tokens) to maximal (full context) yields: minimal : ($\alpha^p=0.82, \alpha^c=0.24$), medium : ($\alpha^p=0.65, \alpha^c=0.58$), maximal : ($\alpha^p=0.85, \alpha^c=0.87$). The increase in CK contribution from minimal to medium context reflects greater reliance on evidence as it becomes available, while maximal context strongly activates both knowledge sources, consistent with supportive and complementary interactions rather than pure suppression of PK.

Geometric stability and separation. The learned parametric and contextual directions are highly stable across resampling, with average directional similarity exceeding 0.9 for both axes. Moreover, the two directions remain well separated: the mean cosine overlap between PK and CK axes is 0.00 across bootstraps. This consistent orthogonality supports the identifiability motivation for a rank-2 formulation. Overall, these results demonstrate that PK-CK disentanglement is stable across layers, robust to prompt surface perturbations, responsive to context evidence, and geometrically well-conditioned.

| Intent | Prompt |
|--------|---|
| w_p | <p>< begin_of_text >< start_header_id >system< end_header_id > Answer the following query considering the provided context. Answer with only one word.< eot_id >< start_header_id >user< end_header_id > Context: Daily Grind Cafe is a popular place to eat lunch out. At a Potluck Party, everyone brings their own lunch to share with friends. Instruction: Ignore the context in answering the query. Query: Which action can help a person save money? A. stop eating at Daily Grind Cafe B. attend a Potluck Party C. Unknown< eot_id >< start_header_id >assistant< end_header_id ></p> |
| w_c | <p>< begin_of_text >< start_header_id >system< end_header_id > Answer the following query considering the provided context. Answer with only one word.< eot_id >< start_header_id >user< end_header_id > Context: Daily Grind Cafe is a popular place to eat lunch out. At a Potluck Party, everyone brings their own lunch to share with friends. Instruction: Only consider the context in answering the query. Query: Which action can help a person save money? A. stop eating at Daily Grind Cafe B. attend a Potluck Party C. Unknown< eot_id >< start_header_id >assistant< end_header_id ></p> |
| w_b | <p>< begin_of_text >< start_header_id >system< end_header_id > Answer the following query considering the provided context. Answer with only one word.< eot_id >< start_header_id >user< end_header_id > Context: Daily Grind Cafe is a popular place to eat lunch out. At a Potluck Party, everyone brings their own lunch to share with friends. Instruction: Consider the context in answering the query. Query: Which action can help a person save money? A. stop eating at Daily Grind Cafe B. attend a Potluck Party C. Unknown< eot_id >< start_header_id >assistant< end_header_id ></p> |

Table 1. Prompt template for intent-driven answer control.

| Intent | Prompt |
|--------|---|
| NLE | <pre>< begin_of_text >< start_header_id >system< end_header_id > Answer the following query considering the provided context. Generate your final answer with only one word. If you are unable to answer the query, generate your final answer as "Unknown". Also, generate an explanation to determine your final answer. Return your output in JSON format: {"explanation": "your explanation here", "answer": "your final response here"}. Only include the JSON object in your response. < eot_id >< start_header_id >user< end_header_id > Context: Daily Grind Cafe is a popular place to eat lunch out. At a Potluck Party, everyone brings their own lunch to share with friends. Query: Which action can help a person save money? A. stop eating at Daily Grind Cafe B. attend a Potluck Party C. Unknown < eot_id >< start_header_id >assistant< end_header_id ></pre> |
| CoT | <pre>< begin_of_text >< start_header_id >system< end_header_id > Answer the following query considering the provided context. Generate your final answer with only one word. If you are unable to answer the query, generate your final answer as "Unknown". Also, generate an explanation to determine your final answer. Return your output in JSON format: {"explanation": "your explanation here", "answer": "your final response here"}. Only include the JSON object in your response. < eot_id >< start_header_id >user< end_header_id > Context: Daily Grind Cafe is a popular place to eat lunch out. At a Potluck Party, everyone brings their own lunch to share with friends. Query: Which action can help a person save money? A. stop eating at Daily Grind Cafe B. attend a Potluck Party C. Unknown < eot_id >< start_header_id >assistant< end_header_id > Give your answer by analyzing step by step.</pre> |

Figure 9. Prompt templates for NLE generation and CoT-based prompting.

| Hyperparameter | Llama | Gemma | Mistral |
|-------------------|-------|-------|---------|
| number of samples | 500 | 200 | 500 |
| batch size | 24 | 10 | 10 |
| τ_p | 0.65 | 0.75 | 0.75 |
| τ_c | 0.60 | 0.85 | 0.65 |
| margin | 0.3 | 0.3 | 0.3 |
| eps | 0.05 | 0.05 | 0.05 |

Figure 10. Patching hyperparameters for identifying important layers for rank-2 projection subspaces from Llama-3.1-8B-Instruct, Gemma-2-9B-it, and Mistral-7B-Instruct-v0.3.

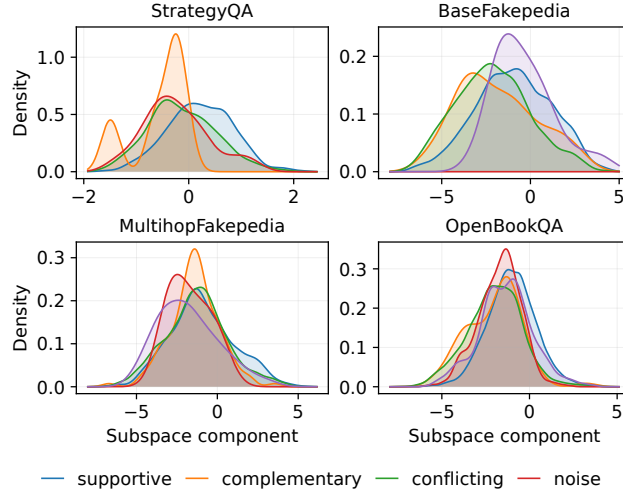


Figure 11. Kernel Density Estimate (KDE) of the PK-CK subspace component $\langle \vec{u}^T, \vec{h}_i \rangle$ across different knowledge interaction types for four question-answer datasets using the Llama-3.1-8B-Instruct model.

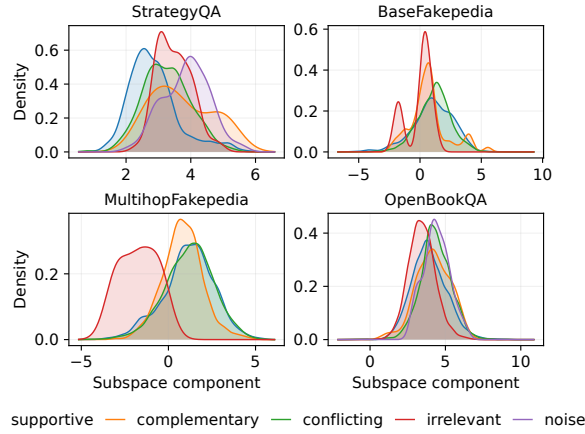


Figure 12. Kernel Density Estimate (KDE) of the PK-CK subspace component $\langle \vec{u}^T, \vec{h}_i \rangle$ across different knowledge interaction types for four question-answer datasets using the gemma-2-9b-it model.

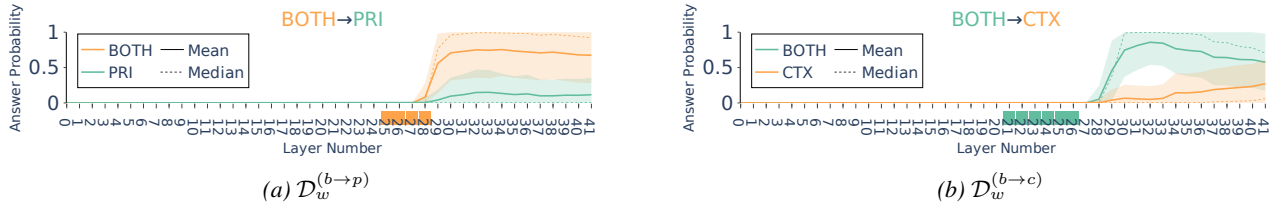


Figure 13. Patchescope on OpenBookQA dataset from gemma-2-9b-it. (a) Activation patching on $\mathcal{D}_w^{(b \rightarrow p)}$ results in a higher contribution of PK in generating the final answer, as the probability gap between the source and target is higher. (b) Activation patching on $\mathcal{D}_w^{(b \rightarrow c)}$ results in a lower contribution of CK in generating the final answer, as the probability gap between the source and target is lower. We consider the common layers from both activation patching to learn the rank-2 projection subspace.

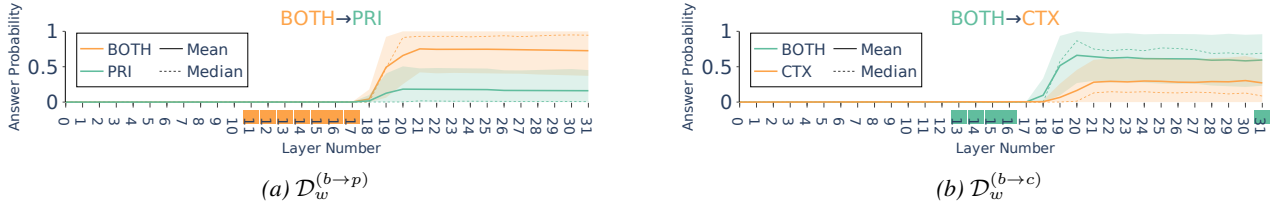


Figure 14. Patchscope on OpenBookQA dataset from Mistral-7B-Instruct-v0.3. (a) Activation patching on $\mathcal{D}_w^{(b \rightarrow p)}$ results in a higher contribution of PK in generating the final answer, as the probability gap between the source and target is higher. (b) Activation patching on $\mathcal{D}_w^{(b \rightarrow c)}$ results in a lower contribution of CK in generating the final answer, as the probability gap between the source and target is lower. We consider the common layers from both activation patching to learn the rank-2 projection subspace.

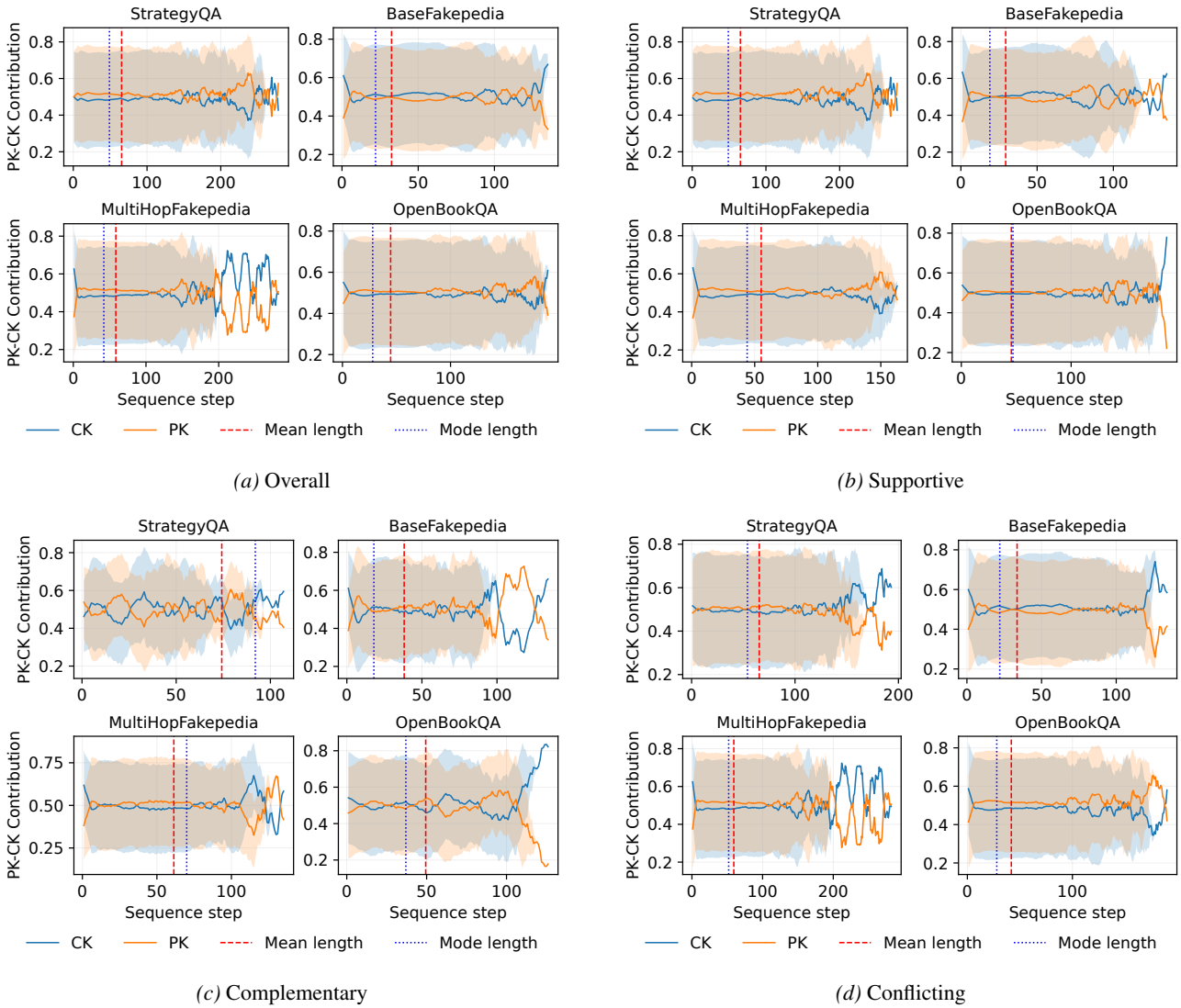


Figure 15. PK-CK interaction dynamics over the sequence steps for different interaction scenarios for Meta-Llama-3.1-8B-Instruct. The dotted red and blue lines indicate the mean and mode of NLE lengths.

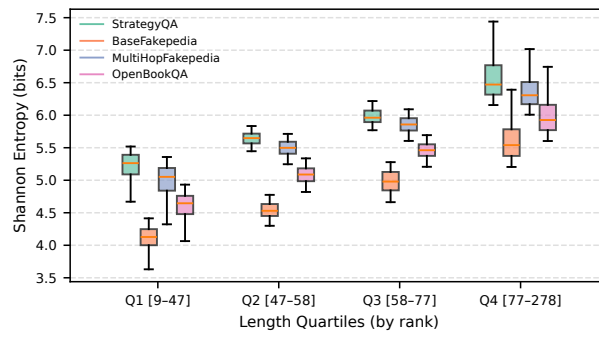


Figure 16. Entropy of NLE generation across all datasets from Meta-Llama-3.1-8B-Instruct for different NLE lengths grouped in four quartiles.